ADVANCES IN GEOPOLYMER SCIENCE & TECHNOLOGY

Alkali-activated metakaolin-slag blends—performance and structure in dependence of their composition

A. Buchwald · H. Hilbig · Ch. Kaps

Abstract Blast furnace slag and metakaolin were blended together and the combination activated by sodium hydroxide solution. The boundary mixtures were set by the activation of the pure slag and pure metakaolin powders. The type and quantity of the reaction products in the alkaline activated blended binders was determined. It is discussed whether both raw materials react separately and are unaffected by each other or if there is a chemical interaction. The discussion bases on extensive investigations with ^{29}Si and ^{27}Al nuclear magnetic resonance spectroscopy compared with X-ray diffraction and thermal analysis (DTA/TG). Additionally, the strength performance will be presented and related to structure, composition and the amount of the reaction products.

Introduction

The term "geopolymer" as used by Davidovits [1] is hardly connected to the reaction of metakaolin with alkaline solutions forming amorphous to semi-crystalline three-dimensional networks by polycondensation [2]. It has been chosen because of its analogy to organic material, which react at ambient temperatures to solid polymers. The prefix "Geo" refers to the inorganic nature of the material.

Apart from metakaolin, several materials react in this way, for instance, thermally treated clays [3], ashes, natural pozzolanes or minerals [4] as well as different waste materials. They have to consist of a metastable or amorphous phase with a high energetic level. In detail, the whole reaction comprises two more or less parallel steps,

1. Activation by an alkaline solution to form reactive monomers or oligomers.
2. Polycondensation to form the aluminosilicate network (ASN).

Geopolymers are alkali-activated materials. Alkaline activation has been used successfully for the activation of blast furnace slag since for more than 40 years [5, 6]. The reaction products of alkali-activated blast furnace slag have been widely investigated and can be compared to calcium silicate hydrates (C-S-H) and calcium aluminate hydrates (C-A-H) from Portland cements, apart from incorporated tetrahedral aluminium into the dreierketten structure of the calcium silicate hydrates [7] and hydrotalcite if the slag contains magnesium [8, 9].

What makes an alkali activation of metakaolin and blast furnace slag so different? Blast furnace slag contains a reasonable amount of calcium inside the glassy phase. If alkali-activated slags do not belong to the group of geopolymers, what happens after mixing slag and metakaolin and then activating with alkaline solution? What kind of reaction product will be formed? It has been shown the possibility of a simultaneously formation of C-S-H and aluminosilicate phases in metakaolin/lime mixtures depends on the

A. Buchwald (✉) · Ch. Kaps
Bauhaus-University Weimar, Weimar, Germany
e-mail: anaj.buchwald@bauing.uni-weimer.de

H. Hilbig
Centre of building materials (cbm), Technical University Munich, Munich, Germany

alkalinity of the system [10]. Yip and van Deventer [11] found in their investigation on metakaolin/slag blends that C-S-H phases and aluminosilicate gel coexist.

The question is whether there is a coexistence of the two types of reaction products? Will there be an interaction between the partners in the blend? Will different reaction products be formed or is there domination of one of the partners, instance e.g. calcium dominates the reaction of the blends and only C-S(A)-H/C-A-H phases will be formed. Are these geopolymers?

It is attempted to answer these questions in this paper by discussing metakaolin-slag blends activated using pure sodium hydroxide solutions.

Experimental

Materials, mixture design and sample preparation

Ground granulated blast furnace slag (S) and commercially available metakaolin Metastar 402 from Imerys GB (M) were used as raw materials. The chemical composition and physical properties are given in Tables 1 and 2. As can seen by the chemical phase compositions in Fig. 1, as well as 73 wt.% glass, the slag used in this work contains crystalline calcium silicate phases and a considerable amount of calcite. Beside the crystalline phases feldspar, quartz and muscovite,

84 wt.% of the metakaolin is amorphous attributed to dehydroxylated kaolinite.

These materials were activated with sodium hydroxide solution in such way that the concentration for the activation of the pure metakaolin was higher than for the pure slag in order to reach the same Na/Al value of 0.4. The water content was adjusted to give the same workability of the pastes; therefore the water content varies. The detailed mixtures are given in Table 3.

Samples measuring $1 \times 1 \times 6$ cm^3 were prepared and kept inside the moulds at 40°C for one day. After de-moulding the samples were stored in closed boxes over water at room temperature.

Strength measurements

Compressive strength and bending tensile strength were measured after 28 days of storage. The measurement of bending tensile strength was performed with three specimens ($1 \times 1 \times 6$ cm^3) of each mixture using three-point bending. The compressive strength was measured on each of the resulting half's of the specimens with a compression area of 1×2 cm^2.

Solid state NMR spectroscopy

Solid state NMR experiments were performed with a Bruker Avance 300 spectrometer (magnetic field strength 7.0455 T, resonance frequency of ^{29}Si and ^{27}Al is 59.63 and 78.20 MHz, respectively). To measure the ^{29}Si MAS NMR spectra, the samples were packed in 7 mm zirconia rotors and spun at 5 kHz at an angle of 54°44′. The chemical shifts were recorded relative to external tetramethylsilane (TMS). The single pulse technique was applied with a pulse width of 4 μs. According to the high paramagnetic portion of the samples, a short repetition time of 5 s was chosen [12] and a typical number of scans were 40,000. For the ^{27}Al MAS NMR spectra the samples were packed in 4 mm zirconia rotors and spun at 15 kHz at an angle of 54°44′. The chemical shifts were recorded relative to external $Al(H_2O)_6^{3+}$. The single pulse technique was used with a pulse width of 3 μs. The repetition time was 2 s and the number of scans was 1,000. Thirty Hertz line broadening was applied to all spectra prior to deconvolution. The signal patterns of the spectra were deconvoluted with the Bruker WINNMR software using Lorentz curve which led to the best result.

X-ray diffraction

To determine the X-ray diffraction pattern the hardened and dried material was mixed with a standard
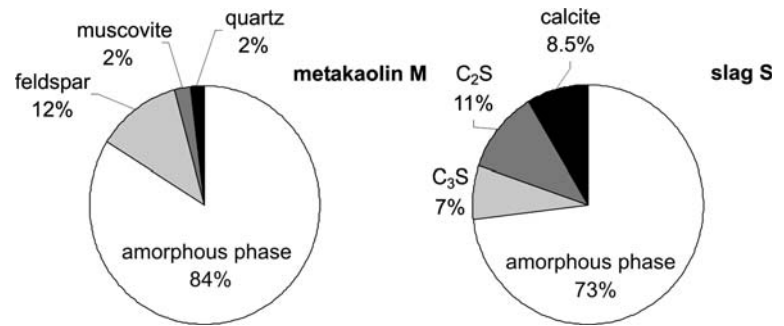
Table 1 Chemical composition of the raw materials

wt.%	Slag	Metakaolin
LOI	4.91	1.0
SiO_2	31.34	52.1
Al_2O_3	10.39	43.0
Fe_2O_3	1.08	0.7
CaO	42.61	0.0
MgO	7.52	0.3
K_2O	0.66	2.5
Na_2O	0.25	0.12
Cl	0.03	ND
SO_3	1.08	ND
P_2O_5	0.13	ND

ND not determined

Table 2 Physical properties of the raw materials

	Density (g/cm^3)	Surface area, measured by		Mean grain size (μm)
		Blaine (cm^2/g)	BET (cm^2/g)	
Slag (S)	2.9	8,120		15.8
Metakaolin (M)	2.55		11,600	3.9

Fig. 1 Mineral composition of the metakaolin and slag

Table 3 Composition of alkali-activated blends

Name/wt%	Metakaolin	Slag	NaOH	Water
AA-M	54.5	0.0	7.1	38.4
AA-M50/S50	31.2	31.2	5.1	32.4
AA-M25/S75	16.8	50.5	3.9	28.7
AA-S	0.0	73.2	2.5	24.4

material (ZnO about 10% per weight) and ground under addition of isopropanol in a bar mill (McCrone-Micronizer, McCrone Ltd., UK) for about 1 min. This mill was used to avoid preferred orientation (texture) and the introduction of stress. CuKα radiation was used. Quantification was carried out using Rietveld refinement (Autoquant®).

Thermal analysis

Thermal analysis was determined in a Seteram Setsys 16/18 equipment under air using a heating rate of 10 K/min in the temperature range 30–1,000°C.

Scanning electron microscopy

Scanning electron microscopy was performed with a HITACHI S2700LB combined with EDS TRACOR Voyager 2100. The experiments were carried out on dried but freshly broken samples that were sputtered with carbon.

Results

Strength

The pure slag binder (AA-S) reached the maximal strength values whereas the pure metakaolin binder (AA-M) showed a low strength which was probably due to the low alkali concentration as can be seen in Fig. 2. The samples of the blends (AA-M50/S50 and AA-M25/S75) achieved similar strength to the pure slag binder. The results of the bending tensile strength
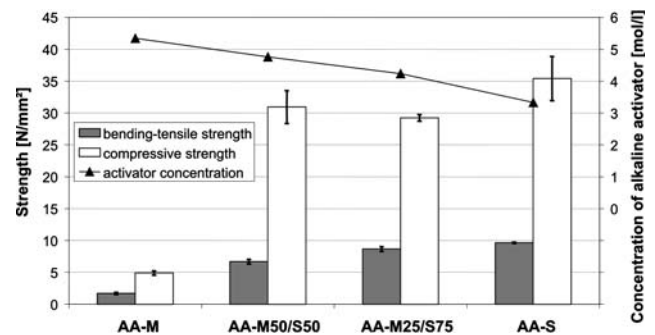

Fig. 2 Strength performance of the alkali-activated blends

follow almost the same trend. The compressive strength of the blend AA-M25/S75 seems to be a little lower than the strength of the blend AA-M50/S50.

Reaction products

XRD

The reacted binders consist, as expected, mostly of amorphous phases either from not reacted raw material or from non-crystalline reaction products (Fig. 3). The crystalline phases quartz, muscovite, feldspar and calcite are supplied by the raw materials. New formed crystalline phases can only be seen in the samples containing slag, instance e.g. hydrotalcite (especially in AA-S) that is commonly found in alkali-activated slags and slag blended cements [8, 9]. The pronounced humps around 30° and 50° 2θ indicate the formation of a small quantity of crystalline C-S-H-phases.

DTA

The results of the thermal analysis are shown in Fig. 4. In the temperature range 30 to 300°C the lost of the different bonded adsorptive water of the binders AA-M and AA-S made with the single powders metakaolin and slag, respectively can be observed. The curves for the blends (AA-M50/S50 and AA-M25/S75) are clearly due to a combination of the curves for the binders

Fig. 3 X-ray diffraction
pattern of the binders
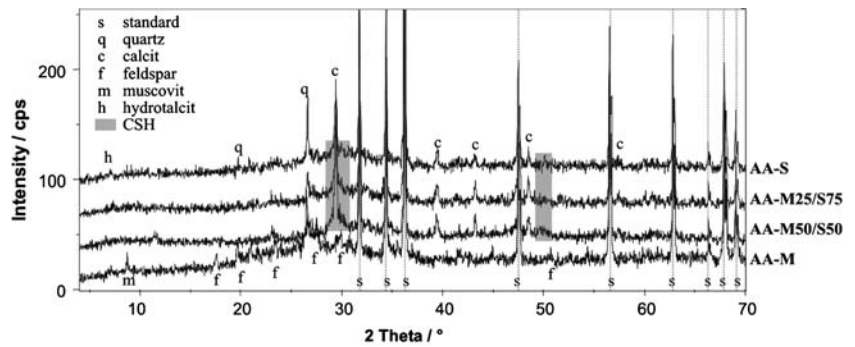
made with the single materials (AA-M and AA-S) without any other contributions.

NMR

The expected structure informations using ^{29}Si NMR spectroscopy are described as follows:

- Silicate tetrahedra which are bonded in silicate chains can either be situated at the chain ends (Q_1; NMR signal at –78 ppm ± 2 ppm) or in the middle (Q_2, NMR signal at –85 ppm ± 2 ppm). If aluminate tetrahedra are incorporated into the silicate chain as bridging tetrahedra, an additional NMR peak from the neighbouring Silicates will appear at –82 ppm ± 2 ppm ($Q_2(1Al)$) [13].
- Zeolites as well as geopolymers are a network of silicate and aluminate tetrahedra that connect over all four corners to other tetrahedra. Therefore five

possible NMR peaks of silicate tetrahedra Q_4, which are connected to zero, one, two, three or four aluminate tetrahedra might be detectable in the spectrum between –85 and –110 ppm [14].

Figure 5 presents the ^{29}Si NMR spectra of the raw materials metakaolin (M) and slag (S) as well as the spectra of the alkali-activated materials (binders AA-M, AA-S, AA-M50/S50, AA-M25/S75). The spectrum of the metakaolin contains one predominant broad single peak with a maximum around –101 ppm from $Q_4(1Al)$. The alkali-activated metakaolin (AA-M) consist of unreacted metakaolin which can be seen on the broad peak at –101 ppm and reaction product which can be seen on several peaks mainly situated in the range between –80 and –93 ppm.

The spectrum for the slag contains one broad peak centred around –74 ppm. The alkali-activated slag (AA-S) comprises still unreacted slag (broad peak at –74 ppm) and reaction product that can be seen as a
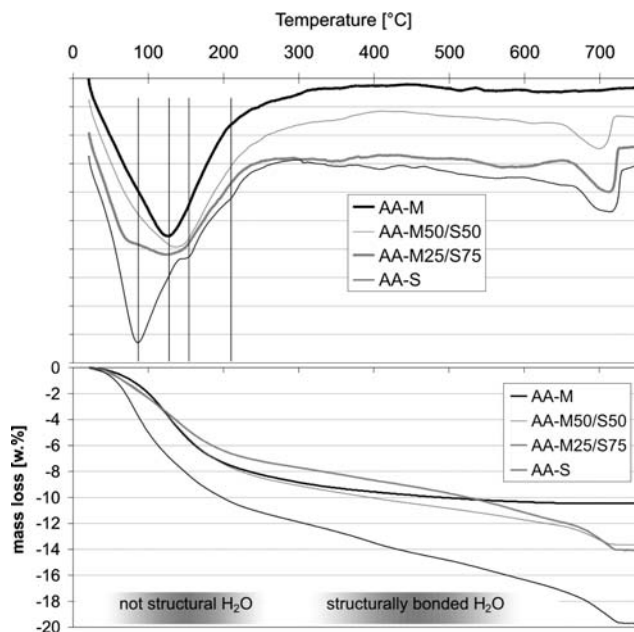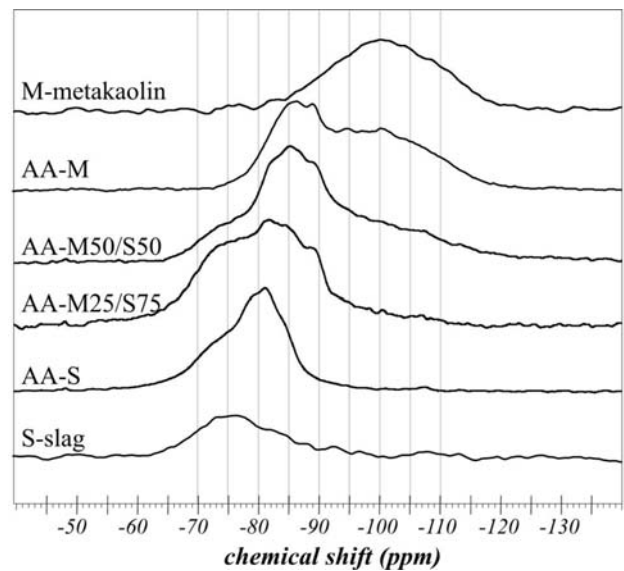

Fig. 4 Results of thermal analysis

Fig. 5 ^{29}Si NMR spectra of the raw materials and alkali-activated binders

broad peak in the range between –75 and –87 ppm. The alkali-activated blends (AA-M50/S50 and AA-M25/S75) show peaks of more or less unreacted slag and metakaolin and peaks of reaction products in the whole range between –75 and –93 ppm.

The ^{27}Al NMR spectrum of a slag binder should show signals of four-coordinated aluminium created by the aluminate tetrahedra incorporated in the silicate chains of the C-S-H-phases [8] as well as signals of six-coordinated aluminium from magnesium or calcium aluminate hydrate phases [15]. The spectrum of the ASN should exhibit only one signal due to the four-coordinated aluminium [10]. Figure 6 shows the ^{27}Al NMR spectra of the raw materials metakaolin (M) and slag (S) as well as the spectra of the alkali-activated materials (binders AA-M, AA-S, AA-M50/S50, AA-M25/S75). The spectrum for the metakaolin contains three overlapping peaks according to four-, five- and six-coordinated aluminium. The AA-M comprises unreacted metakaolin which can be seen by the small peak at 0 ppm (six-coordinated aluminium). The reaction product can be seen as the large peak centred on 60 ppm which comes from the four-coordinated aluminium bonded in the ASN.

The spectrum of the slag shows several broad strongly overlapping peaks according to varying environments of four-, five- and six-coordinated alumin-ium. The AA-S comprises unreacted slag indicated by the asymmetric shape of the tetrahedral aluminium that overlaps the peak of tetrahedral aluminium inside the C-S-H-phases (around 70 ppm). Additionally a reaction product with six-coordinated aluminium is formed which can be seen as the sharp peak at about 10 ppm. Based on the results of X-ray diffraction this signal can be assigned to the hydrotalcite phase.

The alkali-activated blends (AA-M50/S50 and AA-M25/S75) show one dominant peak around 60 ppm, mainly from the tetrahedral aluminium of the ASN. The asymmetric shape indicates the overlapping with tetrahedral aluminium of different environments, for example in the unreacted slag and metakaolin and in the C-S-H-phases.

Quantifying of the reaction products

The NMR spectra were deconvoluted following the regime shown in Fig. 7. First the spectra of the raw materials were evaluated with the Bruker WINNMR Deconvolution software to obtain values for chemical shift, width and intensity of all signals. The peak position and its width were used as fixed values for the next step: The spectra of the alkali-activated binders made from the single materials were evaluated by using the fixed peak position and width from the raw materials to fit the unreacted material using the
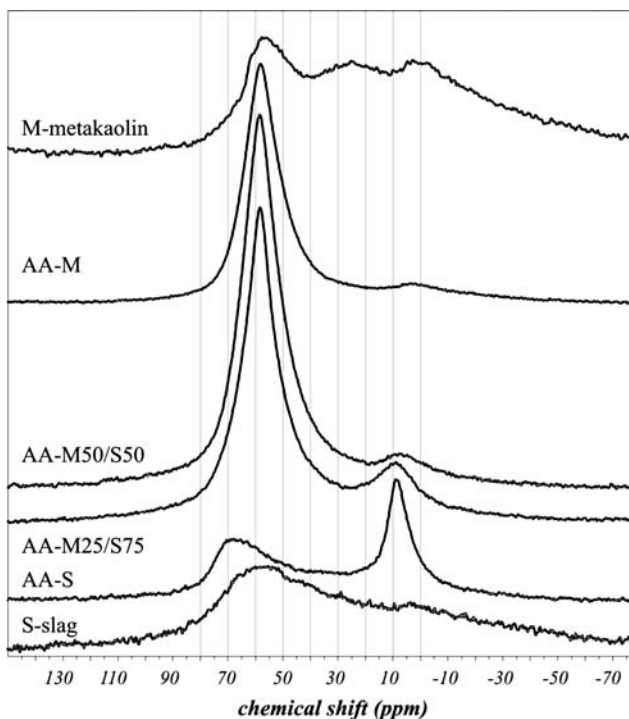

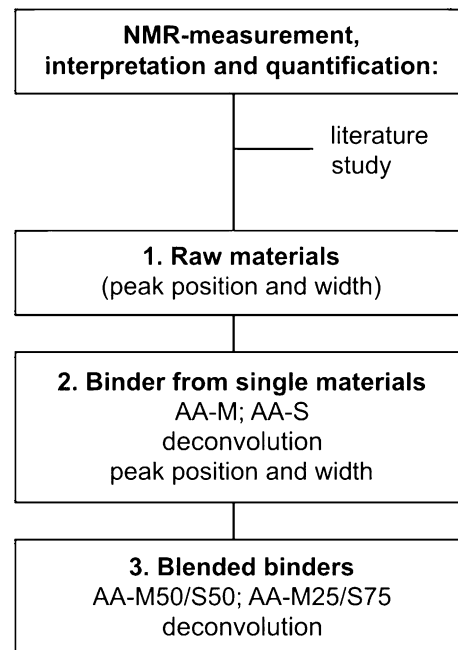Fig. 6 ^{27}Al NMR spectra of the raw materials and alkali-activated binders

Fig. 7 Procedure for the deconvolution and interpretation of the alkali-activated binders

intensity. The literature data as described above were used to define the peak positions and fit the signals of the reaction product with the parameters width and intensity. The peak position and its width were used again as fixed values in the next step: By using the fixed peak positions and widths of the pure binder spectra and fitting only the peak intensity, the deconvolution of the spectra of the alkali-activated blends led to reasonable results.

The results of the deconvolution are shown in Figs. 8, 9, 10, 11, 12.

The intensity of the single peaks was used to calculate the amount G_{Qi} of the different chemical environments of silicon and aluminium.

Difficulties occurred for the deconvolution of both the ^{29}Si NMR and ^{27}Al NMR spectra of the alkali-activated blends because of overlapping peaks at –85 ppm from Q_2 of the C-S-H-phases and Q_4(4Al) of the ASN as well as the overlapping peaks of tetrahedral aluminium in the C-S-H, the ASN and the raw materials. Few preliminary considerations have been made:

- The intensity of the Q_4(4Al)-signal will effect the Si/Al ratio of the ASN quite strongly. The aluminosilicate can not incorporate more aluminium into the network because of the molar value Si/Al is already about 1. It can also not give up any silicon for the same reason.
- The intensity of the Q_2-signal can reach at most the intensity of the Q_2-signal of the pure slag binder. The intensity will decrease if more aluminium is included in the C-S-H-phases.
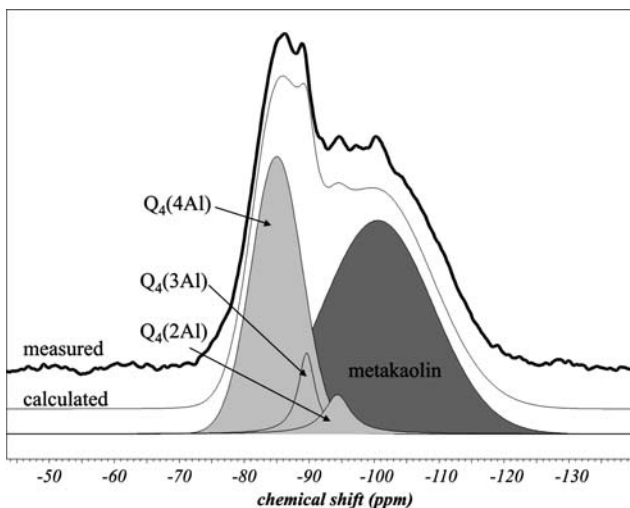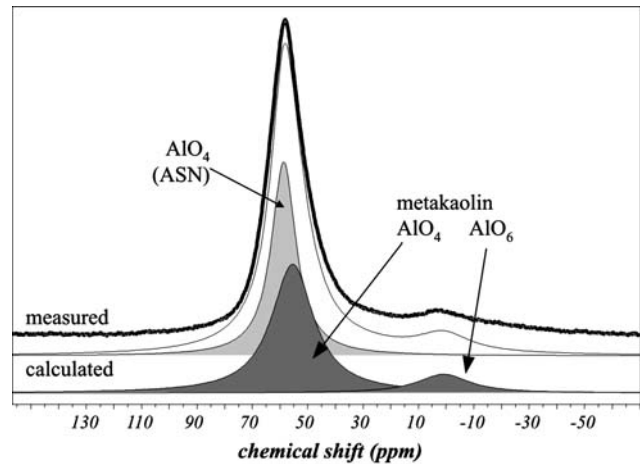

Fig. 9 ^{27}Al NMR spectrum and interpretation of the alkali-activated metakaolin (AA-M)
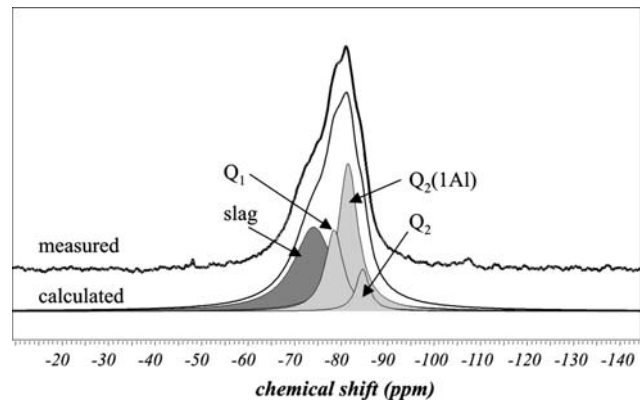

Fig. 10 ^{29}Si NMR spectrum and interpretation of the alkali-activated slag (AA-S)

Fig. 8 ^{29}Si NMR spectrum and interpretation of the alkali-activated metakaolin (AA-M)

Fig. 11 ^{27}Al NMR spectrum and interpretation of the alkali-activated slag (AA-S)
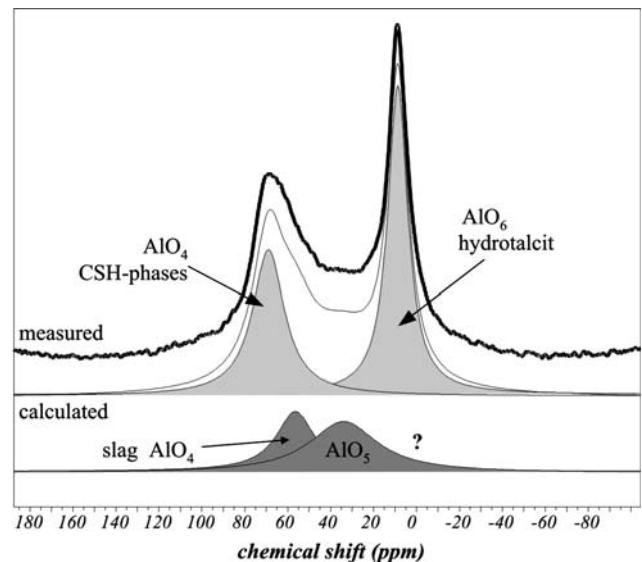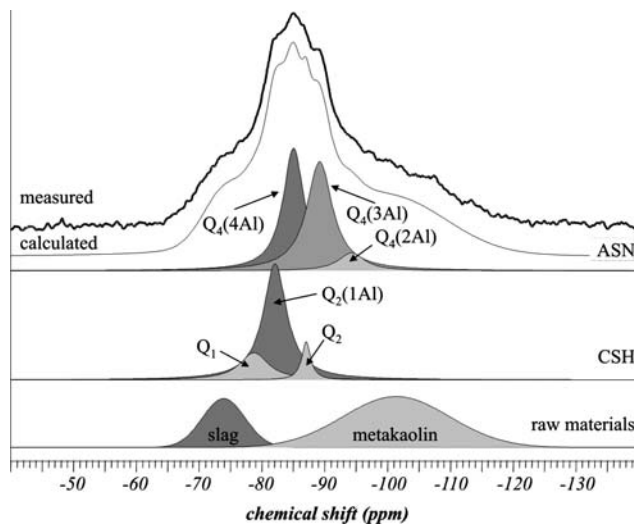
Fig. 12 ^{29}Si NMR spectrum and interpretation of the alkali-activated blend 50% metakaolin/50% slag (AA-M50/S50)

That means that the dominant peak should be the $Q_4(4Al)$-signal from the ASN rather than the Q_2-signal from the C-S-H phases. The calculation of the amounts of aluminosilicate and C-S-H are made by help of the fitting procedure with fixed position and width which has been taken out of the pure metakaolin and slag binder spectra, respectively, as described above. The different environments of tetrahedral aluminium of the alkali-activated blends could not be separated in this way. The results of the ^{29}Si-NMR are in Table 4 and the results of the ^{27}Al-NMR in Table 5.

Due to the large noticeable amount of unreacted raw materials the question on the degree of reaction (RD) arises. These values can be calculated using the amount of unreacted material metakaolin G_M and slag G_S given in Table 4. Therefore the silicon input from metakaolin $X(Si)_M$ and slag $X(Si)_S$, respectively, which is known from chemical und mixture composition, has to be considered. Then the reaction degree of the metakaolin RD_M and the slag RD_S can be calculated as follows:

$$RD_M = \frac{X(Si)_M - G_M(-101\,ppm)}{X(Si)_M}$$

$$\text{and} \quad RD_S = \frac{X(Si)_S - G_S(-74\,ppm)}{X(Si)_S}$$

In this case the reaction degree of each raw material in blends can be discussed separately. The overall reaction degree RD_{ov} can also be calculated directly by using the amount of the reaction products (RP):

$$RD_{ov}(^{29}Si) = \sum_{i=1}^{4} G_{Q_i}(RP)$$

The results are given in Table 6.

Based on the quantification of each signal, the average chain length (CL) and the molar ratio silicon to aluminium of the C-S-H-phases (Si/Al_{C-S-H}) as well as of the ASN (Si/Al_{ASN}) can be calculated:

$$\overline{CL} = \frac{G_{Q_1} + \frac{3}{2}G_{Q_2(1Al)} + G_{Q_2}}{\frac{1}{2}G_{Q_1}}$$

$$Si/Al_{CSH} = \frac{G_{Q_1} + G_{Q_2(1Al)} + G_{Q_2}}{\frac{1}{2}G_{Q_2(1Al)}}$$

Table 4 Results of ^{29}Si NMR spectroscopy

Position G_i/mol-%Si	S −74 ppm	Q_1 −79 ppm in CSH	Q_2(1Al) -81 ppm in CSH	Q_2 −85 ppm in CSH	Q_4(4Al) −84 ppm in ASN	Q_4(3Al) −89 ppm in ASN	Q_4(2Al) −94 ppm in ASN	M −101 ppm
AA-M	0.0	0.0	0.0	0.0	34.7	3.5	3.8	58.0
AA-M50/S50	10.5	5.0	17.6	2.2	16.7	17.9	3.0	27.0
AA-M25/S75	40.3	9.7	17.3	0.8	10.5	11.3	0.4	9.7
AA-S	35.7	30.4	21.8	12.1	0.0	0.0	0.0	0.0

Table 5 Results of ^{27}Al NMR spectroscopy

Position G_i (mol% Al)	AlO$_4$			AlO$_5$	AlO$_6$
	68 ppm in CSH	58 ppm in ASN	56 ppm	30 ppm	10 ppm
S	–	–	52.2	37.3	10.4
M	–	–	20.7	29.0	50.3
AA-M	–	41.3	47.1	2.9	8.7
AA-M50/S50		40.8	49.0	1.7	8.5
AA-M25/S75		35.4	45.0	1.4	18.3
AA-S	27.9	–	13.9	20.9	37.3

Table 6 Specification of the reaction products

	CSH		ASN
	CL	Si/Al	Si/Al
AA-M	–	–	1.07
AA-M50/S50	13.4	2.8	1.19
AA-M25/S75	7.5	3.2	1.16
AA-S	5.0	5.9	–

$$\text{Si/Al}_{ASN} = \frac{\sum_{n=0}^{4} G[Q_4(n\text{Al})]}{\sum_{n=0}^{4} \frac{n}{4} G[Q_4(n\text{Al})]}$$

The results are given in Table 7.

Discussion

The alkaline activated metakaolin (AA-M) reacted to form an ASN showing, as expected, only Q_4-Signals in the ^{29}Si NMR spectrum and four-coordinated aluminium in the ^{27}Al NMR spectrum. The appearance of signals from structures other than the $Q_4(4\text{Al})$ is generally not observed. This can be explained by the low activator concentration as was shown in [16]. The alkaline activated slag (AA-S) reacted to form C-S-H-phases (with incorporated aluminium), revealed as Q_1 and Q_2 in the ^{29}Si NMR spectrum and four-coordinated aluminium in the ^{27}Al NMR spectrum, as well as to hydrotalcite which was seen as six-coordinated aluminium in the ^{27}Al NMR spectrum and confirmed by X-ray diffraction.

At the first, the reaction product of the alkali-activated blends (AA-M50/S50 and AA-M25/S75) seems to be only the sum of the single activated powders. This means no dominance of one partner could be found. Considering the low activator concentration chosen, the dominance of formation of C-S-H phases was expected according to the results of Palomo [10]. However, in this case both partners contributed independently. Even for the alkali-activated blend AA-M25/S75, with the lowest activator concentration of metakaolin in the mix, the reaction degree of the metakaolin is much higher than that of the pure

Table 7 Comparison of reaction degree, calculation from ^{29}Si NMR spectroscopy

mol% Si	RD_M	RD_S	RD_{ov}
AA-M	0.42	–	0.42
AA-M50/S50	0.57	0.72	0.62
AA-M25/S75	0.73	0.37	0.50
AA-S	–	0.64	0.64

activated metakaolin binder (AA-M). Contrary to the investigations of Palomo [10], both materials of the blend possess all ingredients necessary for reaction.

The reason for the essentially parallel reaction may be found in the different time and place of reaction. Metakaolin and the components of the slag may have different kinetics for their dissolution/precipitation. These reactions take place at a nanoscale around the grains.

The coexistence of the both types of reaction products can also be seen in the SEM image (Fig. 13). The SEM image for sample AA-M50/S50 shows a slag grain with reaction layer around it. The element composition is shown for two points, EDX1 from the unreacted grain and EDX2 from the reaction layer. Apart from the problem of the measured volume (contribution from deeper layers), the element composition of spot EDX2 might indicate a lower Si/Al than expected for slag and C-S-H but too high for the ASN.

A closer inspection reveals that there is in fact an interaction between the single powders. Slag incorporates aluminium from the metakaolin as can be seen from the change in molar ratio of silicon to aluminium which decreases from 6 (pure slag binder) to 2.8 (50/50 blend). This causes a longer average chain length which increases from 6 to 13. The simultaneous increase of the Si/Al ration of the ASN from 1.07 to about 1.2 underlines the consistency of the measurement and interpretation. The effect of elongation the silicate
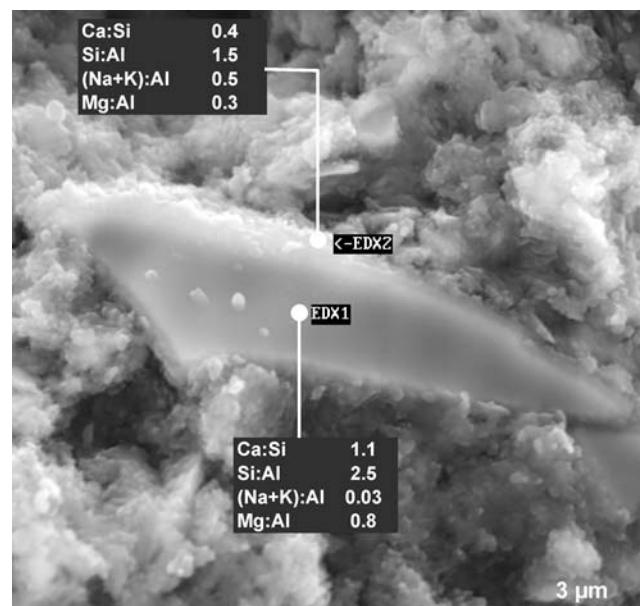

Fig. 13 SEM image and results from EDS measurement of the sample AA-M50/S50

chains in C-S-H by increasing aluminium content was described by Andersen et al. [13] as well. Schneider et al. [17] mentioned the decrease of the molar ratio of silicon to aluminium affected by the increasing sodium hydroxide concentration. As proved in parallel investigation [18], both average chain length and Si/Al ratio remain unaffected by the change of alkaline concentration in a pure slag system. Only the reaction degree could be increased by a higher concentration.

Conclusions

Obviously both type of reaction products—C-S-H from slag and ASN from the metakaolin—are able to coexist. There is only a small interaction between the reacting systems which is probable due to different kinetics of the dissolution process and distribution of the reacting species. The interaction could be shown by the incorporation of additional aluminium into C-S-H phases so that their Si/Al decreased from 6 to 2.8 and their average chain length increased from 6 to 13.

The alkaline activation of metakaolin-slag mixes yields a binder blend containing calcium silicate hydrate system and geopolymer system and a mixture of both phases due to interaction at their contact surfaces. This results in a good overall strength performance.

Whether slag removes the aluminium or the metakaolin cannot retain it due to the low sodium content is not distinguishable. It could not be established whether the different reaction degree was affected by the reaction of the partner or by the change of alkali quantity. Therefore further measurements are in progress at higher and constant activator concentration. In an attempt to bridge the gap of quantification the reaction products from ^{27}Al NMR spectroscopy additional techniques for instance ^{1}H-^{27}Al CP NMR and MQ ^{27}Al NMR will be used.

The results show that the primary question is not "whether these blends are geopolymers or not", but there are binder mixtures containing geopolymer and slag binder in different proportions depending on their composition.

References

1. Davidovits J (1976) In: Proceedings of I.U.P.A.C. international symposium on macromolecules, Stockholm; September 1976; Topic III, New polymers of high stability
2. Davidovits J (1999) In: Davidovits J et al (ed) Proceedings of the 2nd international conference on geopolymer, St. Quentin, p 9
3. Buchwald A, Kaps Ch (2002) In: Grant L (CD) Proceedings of the 3rd international conference on geopolymer, Melbourne, October 2002
4. Hua Xu, van Deventer JSJ (2000) Int J Min Proc 59:247
5. Krivenko PV (2000) In: Stark J (ed) Proceedings of the 14th Ibausil, Weimar, September 2000, p 1-0503
6. Talling B, Brandstetr J (1989) In: Malhotra VM (ed) Proceedings of the 3rd international conference of fly ash, silica fume, slag and natural pozzolans in concrete, p 1519
7. Schilling PJ, Butler LG, Roy A, Eaton HC (1994) J Am Cer Soc 77:2363
8. Richardson IG, Groves GW (1992) J Mater Sci 27:6204
9. Wang SD, Scrivener KL (1995) 25:561
10. Palomo A, Blanco-Valera T, Alonso S, Granizo L (2003) In: Proceedings of the 11th international congress on the chemistry of cement (ICCC), Durban, South Africa, p 425
11. Yip CK, van Deventer JSJ (2003) J Mater Sci 38:3851
12. Dobson CM, Goberdhan DGC, Ramsay JDF, Rodger SA (1988) J Mater Sci 23:4108
13. Andersen MD, Jakobsen HJ, Skibsted J (2003) Inorg Chem 42:2280
14. Davidovits J (1988) In: Proceedings of the 1st international conference on geopolymer, p 149
15. Wang SD, Scrivener KL (2003) Cem Con Res 33:769
16. Singh PS, Trigg M, Burgar I, Bastow T (2002) In: Grant L (CD) (ed) Proceedings of the 3rd international conference on geopolymer, Melbourne, October 2002
17. Schneider J, Cincotto MA, Panepucci H (2001) Cem Con Res 31:993
18. Hilbig H, Buchwald A (2006) J Mater Sci Let 41:6488